Applied Energy 282 (2021) 116090

Contents lists available at ScienceDirect

Applied Energy

journal homepage: www.elsevier.com/locate/apenergy

Distributed planning of electricity and natural gas networks and energy hubs

Hangbo Yang [a], Pengcheng You [b], Ce Shang [a,*]

[a] Ministry of Education Key Laboratory of Control of Power Transmission and Conversion, Department of Electrical Engineering, Shanghai Jiao Tong University, Shanghai 200240, China

[b] Department of Electrical and Computer Engineering, Johns Hopkins University, Baltimore, MD 21218, USA

ARTICLE INFO

Keywords:
ADMM
Distributed optimization
Energy hub
Planning
Unit commitment

ABSTRACT

Centralized planning of the electricity network, natural gas network and energy hubs (EHs) implicitly assumes a vertically integrated structure, which ignores the common independent ownership of different systems. A more practical approach should differentiate the electric system, gas system and each EH as separate stakeholders, and establish a distributed planning framework. Such a distributed planning framework based on the alternating direction method of multipliers (ADMM) is proposed in this paper, which uses the amount of electricity and natural gas required by EHs from each node as the decoupling information, and decomposes the joint planning problem into multiple planning sub-problems, respectively for the electric system, natural gas system and each EH. To reflect the operation more accurately in the planning stage, unit commitment is embedded in the planning model as its operation module. Finally, the proposed method is verified on an illustrative system composed of a modified IEEE RTS 24-bus electric system, Belgian 20-node natural gas system and four EHs. The case study demonstrates the impacts of unit commitment, gas price and penalty parameters on the planning scheme and the number of iterations.

1. Introduction

Coordinating multiple forms of energy in a complementary supply framework, the integrated energy system (IES) has been expected as the future energy solution, which has seen applications in various ranges, from wide-area [1] to regional [2] and community-level [3]. The integrated manner operating multiple energies requires an integrated manner of planning the infrastructure. For wide-area energy integration, therefore, a synergic IES planning framework is actually needed to develop joint expansion strategies of transmission lines, natural gas pipelines and site selections for energy hubs (EHs).

There has been a limited literature on the synergic planning of IES incorporating district EHs in the past few years. It is formulated as a mixed-integer linear program (MILP) [4] and a two-stage MILP model to configure the district EHs [5], which yet both ignore the siting of EHs. However, there has been various work on the synergic planning of part of the systems such as EHs or the electric and gas systems without EHs. Topological layering is adopted to build a multi-layer planning framework of EH [6] to achieve the start-from-scratch planning of EH's internal structure by modeling the EH as a directed acyclic graph (DAG). A synergic planning framework with gas-fired units modeled as coupling devices is proposed [7], ignoring the precise model of the electricity and gas network. Then DC power flow and weymouth steady-state gas flow are adopted to model the electricity and gas network to build a bi-level synergic planning framework [8]. A two-stage stochastic planning [9] is proposed to cope with the uncertainty of load while the investment strategies over the multiple periods in the first-stage cannot be adjusted with the realization of uncertainty, this limitation is addressed in the multi-stage stochastic planning (MSSP) with nonanticipativity constraints [10], and branch-and-price algorithm is further adopted to solve the MSSP more efficiently [11]. Multi-stage robust synergic planning is also proposed to cope with the uncertainties of renewable energy and load [12], N-1 security criterion [13] and system resilience [14]. Although works on the synergic planning is limited, various synergic operation models of IES with EHs have been widely studied, e.g., scheduling of IES incorporating districted EHs [15], bi-level scheduling of IES incorporating district heating systems [16] and optimal energy flow of gas-electric integrated systems [17].

It is commonly assumed in the existing studies of synergic planning that the electric system, natural gas system and EHs all belong to a single stakeholder, who possesses the global information of the systems to make investment and operation decisions. While the single stakeholder planning framework is not practicable in the cases that the three systems are independent of each other, which requires a distributed optimization framework to differentiate them as independent stakeholders. However, a holistic distributed planning or scheduling

* Corresponding author.
E-mail address: shangce@sjtu.edu.cn (C. Shang).

https://doi.org/10.1016/j.apenergy.2020.116090
Received 24 June 2020; Received in revised form 17 October 2020; Accepted 22 October 2020
Available online 16 November 2020
0306-2619/

Nomenclature

Parameters

A	Bus-unit incidence matrix, $A_{n,i} = 1$ if unit i is connected to the bus n
B	Bus-branch incidence matrix, $B_{n,l} = 1$ if transmission line l starts from bus n, $B_{n,l} = -1$ if transmission line l ends at bus n
C	Node-gas source incidence matrix, $C_{m,w} = 1$ if gas source w is connected to the node m
D	Node-pipeline incidence matrix, $D_{m,p} = 1$ if pipeline p starts from node m, $D_{m,p} = -1$ if pipeline p ends at node m
H	Node-compressor incidence matrix, same with **D**
J	Node-gas storage incidence matrix, $J_{m,s} = 1$ if gas storage s is connected to the node m
$\overline{cf}_c$	Capacity of compressor c
$\overline{pf}_l$	Capacity of transmission line l
$\overline{P}_s^{\mathrm{ch}}$, $\overline{P}_s^{\mathrm{dc}}$	Maximum charge and discharge rate of gas storage s
seg	Number of segments in piecewise linearization of Weymouth
$\underline{P}_i^{\mathrm{e}}, \overline{P}_i^{\mathrm{e}}$	Minimum and maximum output limits of unit i
$\underline{\pi}_m$, $\overline{\pi}_m$	Minimum and maximum pressure of gas node m
$\underline{gf}_p$, $\overline{gf}_p$	Minimum and maximum gas flow in pipeline p
$\underline{P}_{ehc}^{\mathrm{in}}$, $\overline{P}_{ehc}^{\mathrm{in}}$	Minimum and maximum input of EH component
$\underline{P}_w^{\mathrm{g}}$, $\overline{P}_w^{\mathrm{g}}$	Minimum and maximum output limits of gas source w
ς_c	Compression factor of compressor c
b_l	Susceptance of transmission line l
$L_{j,t}^{\mathrm{e}}$	Electricity load of EH j in hour t
$L_{j,t}^{\mathrm{g}}$	Natural gas load of EH j in hour t
$L_{j,t}^{\mathrm{h}}$	Heat load of EH j in hour t
$L_{m,t}^{\mathrm{g}}$	Natural gas load at node m in hour t
$L_{n,t}^{\mathrm{e}}$	Electricity load at bus n in hour t
RU_i, RD_i	Ramp-up rate and ramp-down rate of unit i
TU_i, TD_i	Minimum uptime and minimum down time of unit i
w_p	Coefficient of pipeline p
$\eta_{\mathrm{chp}}^{\mathrm{ge}}$	Energy conversion efficiency of CHP from gas to electricity
$\eta_{\mathrm{chp}}^{\mathrm{gh}}$	Energy conversion efficiency of CHP from gas to heat
$\eta_{\mathrm{eb}}^{\mathrm{eh}}$	Energy conversion efficiency of boilers
$\eta_{\mathrm{p2g}}^{\mathrm{eg}}$	Energy conversion efficiency of P2G devices
η_s^{ch}	Charge efficiency of gas storage s
η_s^{dc}	Discharge efficiency of gas storage s
ELC_n	Investment cost of EH at electric node n
GC_i	Generation cost of unit i
GLC_n	Investment cost of EH at gas node m
LC_l	Investment cost of candidate transmission line l
NC_w	Natural gas cost of gas source w
PC_p	Investment cost of candidate pipeline p
SC_i	Startup cost of unit i

Sets and indices

$c \in \Omega_{\mathrm{COM}}$	Compressors
$j \in \Omega_{\mathrm{EH}}$	Energy hubs
$m \in \Omega_{\mathrm{GN}}$	Natural gas nodes
$n \in \Omega_{\mathrm{EN}}$	ELectric nodes
$s \in \Omega_{\mathrm{GS}}$	Gas storages
Ω_{CL}	Set of candidate transmission lines
Ω_{CP}	Set of candidate gas pipelines
Ω_{EL}	Set of existing transmission lines
Ω_{EP}	Set of existing gas pipelines
Ω_{GEN}	Set of units
Ω_{GW}	Set of natural gas sources

Variables

$cf_{c,t}$	Gas flow in compressor c in hour t
$gf_{p,t}$	Gas flow in pipeline p in hour t
$P_{i,t}^{\mathrm{e}}$	Production of unit i in hour t
$P_{m,j,t}^{\mathrm{hfg}}$	Natural gas that EH j obtained from the gas node m in hour t
$P_{n,j,t}^{\mathrm{hfe}}$	Electricity that EH j obtained from the electric node n in hour t
$P_{s,t}^{\mathrm{ch}}$	Gas charge rate of gas storage s in hour t
$P_{s,t}^{\mathrm{dc}}$	Gas discharge rate of gas storage s in hour t
$P_{w,t}^{\mathrm{g}}$	Production of gas source w in hour t
$P_{\mathrm{chp},j,t}^{\mathrm{e,out}}$	Electricity production of CHP of EH j in hour t
$P_{\mathrm{chp},j,t}^{\mathrm{h,out}}$	Heat production of CHP of EH j in hour t
$P_{\mathrm{chp},j,t}^{\mathrm{in}}$	Input of CHP of EH j in hour t
$P_{\mathrm{eb},j,t}^{\mathrm{in}}$	Input of boiler of EH j in hour t
$P_{\mathrm{eb},j,t}^{\mathrm{out}}$	Output of boiler of EH j in hour t
$P_{\mathrm{FN},j,t}^{\mathrm{e}}$	Electricity transmitted from the electric network to EH j's output side in hour t
$P_{\mathrm{FN},j,t}^{\mathrm{g}}$	Natural gas transmitted from the gas network to EH j's output side in hour t
$P_{\mathrm{p2g},j,t}^{\mathrm{in}}$	Input of p2g of EH j in hour t
$P_{\mathrm{P2G},j,t}^{\mathrm{out}}$	Output of P2G of EH j in hour t
$pf_{l,t}$	Power flow on transmission line l in hour t
$s_{m,j}^{\mathrm{g}}$	Binary variables, taking the value of 1 of EH j is connected to the gas m

of IES with district EHs is still missing. Though several references have differentiated part of the three systems as separate stakeholders in decision-making, such as distributed planning of the electric system and natural gas system [18]. Despite the lack of distributed planning, the distributed operation of IES has been studied, a standard and a consensus-based ADMM approaches are proposed to build the distributed scheduling framework [19] of the electric-gas system to differentiate the two systems as independent stakeholders, then an ADMM based robust distributed scheduling framework [20] is proposed to cope with the uncertainty of electrical load and renewable energy. A distributed optimal energy flow model for multiple EHs [21] is proposed in which the different district EHs are assigned as separate entities. Some works also regard the multi-regional electric-gas system as one stakeholder and district EHs as another, e.g. the deterministic dis-

$s^{\mathrm{e}}_{n,j}$	Binary variables, taking the value of 1 of EH j is connected to the electric node n
$Soc_{s,t}$	Natural gas of gas storage s in hour t
$u_{i,t}$	Binary variables of commitment of unit i in hour t, taking the value of 1 if committed
$v_{i,t}$	Binary variables of startup of unit i in hour t, taking the value of 1 if started up
$w_{i,t}$	Binary variables of shutdown of unit i in hour t, taking the value of 1 if shut down
z_l	Binary variables indicating the investment status of candidate transmission line l
z_p	Binary variables indicating the investment status of candidate pipeline p
$\pi_{m,t}$	Nodal pressure of gas node m in hour t
$\theta_{n,t}$	Phase angle of electric node n in hour t

tributed scheduling [22] and adaptive robust distributed planning [23] of multi-stakeholder IES.

Alternating direction method of multipliers (ADMM) based distributed optimization framework [24] has been popular to handle global problems with coordinated local efforts in multi-agent systems. ADMM generally relaxes the continuous equality coupling constraints to decompose the primal problem into multiple independent sub-problems (the variables and constraints of one sub-problem will not occur in others) with dual multipliers and is known for robust convergence. However, the coupling siting constraints in the joint planning problem would introduce binary variables in the multipliers update, which might significantly degrade its convergence performance. Instead, in this paper the problem is decoupled by relaxing the power and gas balance constraints at each EH-node interface, which still sticks to the relaxation of continuous constraints and keeps the binary siting variables in the subproblems.

Unit commitment (UC), in which the precise security and real short-term operation constraints as well as units' status are modeled, has been employed as the operation strategy in the electric system planning [25] to more accurately represent the system operation and improve the operational flexibility and economy in the planning stage. Convex relaxation [26] is adopted to reduce the computational burden introduced by the binary variables representing the commitment status of units, e.g. in use, start up and shut down, in the UC embedded multi-period planning problem. IES enhances the interactions among various energy forms. The gas factors, e.g., natural gas price, production and pipeline investment strategies will implicitly affect the production of units. It is hence necessary to embed UC in the IES planning framework to reflect more accurate operation in the planning stage as well as improve the operational flexibility.

A UC-embedded distributed IES planning model based on ADMM is proposed in this paper, in which the planning of the electricity and natural gas networks and the siting of EHs are achieved simultaneously. The main contributions of this paper are summarized as follows:

(1) A fully (n+2)-agent (assuming n EHs) distributed planning framework, in which the electric system, the natural gas system and each EH are assigned as different stakeholders simultaneously, is proposed in this paper.
(2) Distributed siting is addressed by representing EHs' site by the energy flow between EHs and the multi-energy networks, which are defined as continuous coupling variables to update the Lagrange multipliers in ADMM.
(3) UC is embedded in the proposed distributed IES planning as an optimized operation strategy to more accurately model the system operation in the planning stage and improve the operational flexibility and economy.

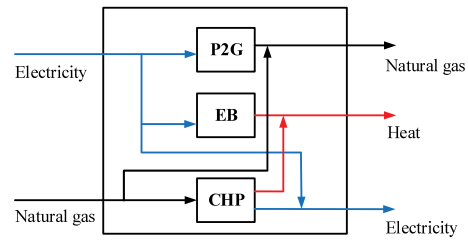

Fig. 1. The configuration of energy hub.

The rest of the paper is organized as follows. The IES equipment model is introduced in Section 2. The synergic centralized and distributed planning framework of IES are formulated as MILP, respectively, in Sections 3 and 4. Case studies are conducted in Section 5. Section 6 concludes the paper.

2. IES equipment model

2.1. Energy hub

The configuration of EHs is shown in Fig. 1, where every EH transforms electricity and natural gas to electricity, gas and heat to meet the multi-energy load in its output port. The components include the combined heat and power (CHP), the power to gas (P2G) and the electric boiler (EB).

(1) Combined heat and power (CHP) units: CHP units convert natural gas into electricity and heat, and the relationship between the input and output of the CHP in EH j is:

$$P^{\mathrm{h,out}}_{\mathrm{chp},j,t} = \eta^{\mathrm{gh}}_{\mathrm{chp}} P^{\mathrm{in}}_{\mathrm{chp},j,t}, \forall j \in \Omega_{\mathrm{EH}}, \forall t, \tag{1}$$

$$P^{\mathrm{e,out}}_{\mathrm{chp},j,t} = \eta^{\mathrm{ge}}_{\mathrm{chp}} P^{\mathrm{in}}_{\mathrm{chp},j,t}, \forall j \in \Omega_{\mathrm{EH}}, \forall t, \tag{2}$$

where the energy conversion efficiency of EH components is considered as constants.

(2) Electric boiler (EB): The EB converts electricity into heat, and the relationship between its input and output is:

$$P^{\mathrm{out}}_{\mathrm{eb},j,t} = \eta^{\mathrm{eh}}_{\mathrm{eb}} P^{\mathrm{in}}_{\mathrm{eb},j,t}, \forall j \in \Omega_{\mathrm{EH}}, \forall t. \tag{3}$$

(3) Power to gas (P2G) units: P2G units convert power into natural gas, and the relationship between the input and output of the P2G in EH j is:

$$P^{\mathrm{out}}_{\mathrm{p2g},j,t} = \eta^{\mathrm{eg}}_{\mathrm{p2g}} P^{\mathrm{in}}_{\mathrm{p2g},j,t}, \forall j \in \Omega_{\mathrm{EH}}, \forall t. \tag{4}$$

Besides, the input constraint of EH components is:

$$\underline{P}^{\mathrm{in}}_{ehc} \le P^{\mathrm{in}}_{ehc,j,t} \le \overline{P}^{\mathrm{in}}_{ehc}, \forall ehc \in \{\mathrm{chp}, \mathrm{eb}, \mathrm{p2g}\}, \forall j \in \Omega_{\mathrm{EH}}, \forall t. \tag{5}$$

(4) Energy balance in output port EHs: EHs must meet the electricity, heat and gas load on the output side, and the constraints are as follows:

$$P^{\mathrm{e,out}}_{\mathrm{chp},j,t} + P^{\mathrm{e}}_{\mathrm{FN},j,t} - L^{\mathrm{e}}_{j,t} = 0, \forall j \in \Omega_{\mathrm{EH}}, \forall t, \tag{6}$$

$$P^{\mathrm{h,out}}_{\mathrm{chp},j,t} + P^{\mathrm{out}}_{\mathrm{eb},j,t} - L^{\mathrm{h}}_{j,t} = 0, \forall j \in \Omega_{\mathrm{EH}}, \forall t, \tag{7}$$

$$P^{\mathrm{out}}_{\mathrm{p2g},j,t} + P^{\mathrm{g}}_{\mathrm{FN},j,t} - L^{\mathrm{g}}_{j,t} = 0, \forall j \in \Omega_{\mathrm{EH}}, \forall t. \tag{8}$$

2.2. Electricity transmission network

Electricity network constraints include the nodal power balance (9), power flow constraints for existing and candidate transmission lines (10)–(14), and phase angle constraints (15). For simplicity, DC power flow is adopted to model the electricity network, and its constraints for existing and candidate transmission lines are shown in (10)–(14), where $\theta^{\mathrm{s}}_{l,t}$ and $\theta^{\mathrm{e}}_{l,t}$ represent the phase angle of transmission line l's start node

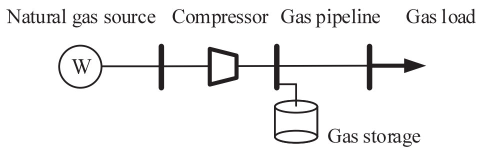

Fig. 2. An example of natural gas system.

and end node. M_{E} is set $2\pi \times b_{l,\max}$ to ensure the power flow on non-built lines to be zero, where $b_{l,\max}$ is the largest susceptance of candidate transmission lines.

$$\sum_{i\in\Omega_{\mathrm{GEN}}} A_{n,i}P^{\mathrm{e}}_{i,t} - \sum_{j\in\Omega_{\mathrm{EH}}} P^{\mathrm{hfe}}_{n,j,t} - L^{\mathrm{e}}_{n,t} + \sum_{l\in\Omega_{\mathrm{EL}}} B_{n,l}pf_{l,t} + \sum_{l\in\Omega_{\mathrm{CL}}} B_{n,l}pf_{l,t} = 0, \forall n \in \Omega_{\mathrm{EN}}, \forall t, \tag{9}$$

$$pf_{l,t} = (\theta^{\mathrm{e}}_{l,t} - \theta^{\mathrm{s}}_{l,t})b_l, \forall l \in \Omega_{\mathrm{EL}}, \tag{10}$$

$$-\overline{pf}_l \le pf_{l,t} \le \overline{pf}_l, \forall l \in \Omega_{\mathrm{EL}}, \forall t, \tag{11}$$

$$pf_{l,t} - (\theta^{\mathrm{e}}_{l,t} - \theta^{\mathrm{s}}_{l,t})b_l - M_{\mathrm{E}}(1 - z_l) \le 0, \forall l \in \Omega_{\mathrm{CL}}, \forall t, \tag{12}$$

$$-pf_{l,t} + (\theta^{\mathrm{e}}_{l,t} - \theta^{\mathrm{s}}_{l,t})b_l - M_{\mathrm{E}}(1 - z_l) \le 0, \forall l \in \Omega_{\mathrm{CL}}, \forall t, \tag{13}$$

$$-\overline{pf}_l \cdot z_l \le pf_{l,t} \le \overline{pf}_l \cdot z_l, \forall l \in \Omega_{\mathrm{CL}}, \forall t, \tag{14}$$

$$-\pi \le \theta_{n,t} \le \pi, \forall n \in \Omega_{\mathrm{EN}}, \forall t. \tag{15}$$

2.3. Natural gas system

The natural gas system is mainly composed of natural gas sources, gas storages, compressors, gas pipelines and gas loads, as in Fig. 2.

(1) Natural gas sources: the production of gas sources is affected by environment and mining technologies, (16) ensures that the natural gas production is within a reasonable range,

$$\underline{P}^{\mathrm{g}}_w \le P^{\mathrm{g}}_{w,t} \le \overline{P}^{\mathrm{g}}_w, \forall w \in \Omega_{\mathrm{GW}}, \forall t. \tag{16}$$

(2) Compressors: The compressor pressurizes the natural gas to cope with the energy loss during the transmission,

$$\pi_{\mathrm{e},t} \le \varsigma_c \pi_{\mathrm{s},t}, \forall c \in \Omega_{\mathrm{COM}}, \forall t, \tag{17}$$

$$0 \le cf_{c,t} \le \overline{cf}_c, \forall c \in \Omega_{\mathrm{COM}}, \forall t. \tag{18}$$

The compressor model is shown in (17), in which the natural gas consumption of the compressor is ignored. (18) is the capacity constraint for compressors.

(3) Gas storage: The gas storages can serve as the natural gas source or load to smooth the load curve and improve the operational flexibility and economy. Constrains (19)–(21) ensure the charge and discharge rate and the natural gas stored in the gas storage in the reasonable range. The natural gas stored in the gas storage in hour t is shown in (22). Constraint (23) predefines the natural gas stored in the gas storages in the final hour of the period to be the same as the initial level to achieve the sustainable use of gas storage.

$$0 \le P^{\mathrm{ch}}_{s,t} \le \overline{P}^{\mathrm{ch}}_s, \forall s \in \Omega_{\mathrm{GS}}, \forall t, \tag{19}$$

$$0 \le P^{\mathrm{dc}}_{s,t} \le \overline{P}^{\mathrm{dc}}_s, \forall s \in \Omega_{\mathrm{GS}}, \forall t, \tag{20}$$

$$\underline{Soc}_s \le Soc_{s,t} \le \overline{Soc}_s, \forall s \in \Omega_{\mathrm{GS}}, \forall t, \tag{21}$$

$$Soc_{s,t} = Soc_{s,t-1} + \eta^{\mathrm{ch}}_s * P^{\mathrm{ch}}_{s,t} - \frac{P^{\mathrm{dc}}_{s,t}}{\eta^{\mathrm{dc}}_s}, \forall s \in \Omega_{\mathrm{GS}}, \tag{22}$$

$$Soc_{s,0} = Soc_{s,\mathrm{T}}, \forall s \in \Omega_{\mathrm{GS}}. \tag{23}$$

(4) Natural gas network: Natural gas network constraints include the nodal gas balance (24), gas flow constraints (25)–(29), and nodal pressure constraints (30). Weymouth steady-state gas transmission model is adopted, in which the relationship between the gas flow and the nodal pressure of existing and candidate pipelines is shown in (25)–(27). M_{G} is a large positive integer in Big-M method to ensure the gas flow on non-built pipelines to be zero.

$$\sum_{w\in\Omega_{\mathrm{GAS}}} C_{m,w}P^{\mathrm{g}}_{w,t} - \sum_{j\in\Omega_{\mathrm{EH}}} P^{\mathrm{hfg}}_{m,j,t} - L^{\mathrm{g}}_{m,t} + \sum_{p\in\Omega_{\mathrm{EP}}} D_{m,p}gf_{p,t} + \sum_{p\in\Omega_{\mathrm{CP}}} D_{m,p}gf_{p,t} + \sum_{c\in\Omega_{\mathrm{COM}}} H_{m,c}cf_{c,t} + \sum_{s\in\Omega_{\mathrm{GS}}} J_{m,s}(P^{\mathrm{dc}}_{s,t} - P^{\mathrm{ch}}_{s,t}) = 0, \forall m \in \Omega_{\mathrm{GN}}, \forall t, \tag{24}$$

$$|gf_{p,t}|gf_{p,t} = w_p(\pi^2_{\mathrm{e},t} - \pi^2_{\mathrm{s},t}), \forall p \in \Omega_{\mathrm{EP}}, \forall t, \tag{25}$$

$$|gf_{p,t}|gf_{p,t} - w_p(\pi^2_{\mathrm{e},t} - \pi^2_{\mathrm{s},t}) - M_{\mathrm{G}}(1 - z_p) \le 0, \forall p \in \Omega_{\mathrm{CP}}, \forall t, \tag{26}$$

$$-|gf_{p,t}|gf_{p,t} + w_p(\pi^2_{\mathrm{e},t} - \pi^2_{\mathrm{s},t}) - M_{\mathrm{G}}(1 - z_p) \le 0, \forall p \in \Omega_{\mathrm{CP}}, \forall t, \tag{27}$$

$$\underline{gf}_p \le gf_{p,t} \le \overline{gf}_p, \forall p \in \Omega_{\mathrm{EP}}, \forall t, \tag{28}$$

$$\underline{gf}_p \cdot z_p \le gf_{p,t} \le \overline{gf}_p \cdot z_p, \forall p \in \Omega_{\mathrm{CP}}, \forall t, \tag{29}$$

$$\underline{\pi}_m \le \pi_{m,t} \le \overline{\pi}_m, \forall m \in \Omega_{\mathrm{GN}}, \forall t. \tag{30}$$

3. Synergic IES planning

The synergic centralized network planning of IES incorporating district EHs can get the global optimal investment and operation strategy, which is a benchmark to verify the effectiveness of the proposed distributed planning model.

3.1. UC-embedded planning

The IES planning framework relies on its operation on a typical day, for which UC is employed to more accurately represent the system operation in the planning. UC constraints consist of units' production constraints (31), ramp rate constraints (32) and (33), minimum up and downtime constraints (34) and (35), and the logic constraint (36) that reflects the impact of startup/shutdown actions on the status of units.

$$u_{i,t}\underline{P}^{\mathrm{e}}_i \le P^{\mathrm{e}}_{i,t} \le u_{i,t}\overline{P}^{\mathrm{e}}_i, \forall i \in \Omega_{\mathrm{GEN}}, \forall t, \tag{31}$$

$$P^{\mathrm{e}}_{i,t} - P^{\mathrm{e}}_{i,t-1} \le RU_i, \forall i \in \Omega_{\mathrm{GEN}}, \forall t \ge 1, \tag{32}$$

$$-P^{\mathrm{e}}_{i,t} + P^{\mathrm{e}}_{i,t-1} \le RD_i, \forall i \in \Omega_{\mathrm{GEN}}, \forall t \ge 1, \tag{33}$$

$$\sum_{tt=t-TU_i+1}^{t} v_{i,tt} \le u_{i,t}, \forall i \in \Omega_{\mathrm{GEN}}, \forall t \in [TU_i, T], \tag{34}$$

$$\sum_{tt=t-TD_i+1}^{t} w_{i,tt} \le 1 - u_{i,t}, \forall i \in \Omega_{\mathrm{GEN}}, \forall t \in [TD_i, T], \tag{35}$$

$$u_{i,t} - u_{i,t-1} = v_{i,t} - w_{i,t}, \forall i \in \Omega_{\mathrm{GEN}}, \forall t, \tag{36}$$

where (34) and (35) also imply that a unit cannot start up and shut down simultaneously: it can be obtained from (34) that $v_{i,t} \le u_{i,t}$, and $w_{i,t} \le 1 - u_{i,t}$ from (35), respectively, which combine to become $v_{i,t} + w_{i,t} \le 1$ [27].

UC, introducing lots of binary variables to more accurately represent the commitment status of units, will introduce significant computational burden, especially in the multi-period planning problems since the planning strategies will be verified on several typical days. Though the strategies to reduce this computational burden are beyond the scope of this paper, the optimal solution of the single-period planning framework proposed in this paper can be obtained in a short period of time.

3.2. EH siting

The binary variable $s^{\mathrm{e}}_{n,j}$ is set to 1 if EH j is connected to node n in the electric system and is set to 0 otherwise; $s^{\mathrm{g}}_{m,j}$ with the gas system is defined similarly. It is assumed that every EH can only be connected to one single node in the electric and the gas system in (37),(40). The electricity and gas consumption of EH j in hour t are shown in (39) and (42). Constraints (38) and (41) ensure the energy obtained from the disconnected node to be zero, where $\overline{P}^{\mathrm{e}}_{\mathrm{h}}$ and $\overline{P}^{\mathrm{g}}_{\mathrm{h}}$ are the EHs' electricity and gas input capacity, respectively.

$$\sum_{n\in\Omega_{\mathrm{EN}}} s^{\mathrm{e}}_{n,j} \le 1, \forall j \in \Omega_{\mathrm{EH}}, \tag{37}$$

$$0 \le P^{\mathrm{hfe}}_{n,j,t} \le s^{\mathrm{e}}_{n,j}\overline{P}^{\mathrm{e}}_{\mathrm{h}}, \forall n \in \Omega_{\mathrm{EN}}, \forall j \in \Omega_{\mathrm{EH}}, \forall t, \tag{38}$$

$$\sum_{n\in\Omega_{\mathrm{EN}}} P^{\mathrm{hfe}}_{n,j,t} = P^{\mathrm{in}}_{\mathrm{eb},j,t} + P^{\mathrm{in}}_{\mathrm{p2g},j,t} + P^{\mathrm{e}}_{\mathrm{FN},j,t}, \forall j \in \Omega_{\mathrm{EH}}, \forall t, \tag{39}$$

$$\sum_{m\in\Omega_{\mathrm{GN}}} s^{\mathrm{g}}_{m,j} \le 1, \forall j \in \Omega_{\mathrm{EH}}, \tag{40}$$

$$0 \le P^{\mathrm{hfg}}_{m,j,t} \le s^{\mathrm{g}}_{m,j}\overline{P}^{\mathrm{g}}_{\mathrm{h}}, \forall m \in \Omega_{\mathrm{GN}}, \forall j \in \Omega_{\mathrm{EH}}, \forall t, \tag{41}$$

$$\sum_{m\in\Omega_{\mathrm{GN}}} P^{\mathrm{hfg}}_{m,j,t} = P^{\mathrm{in}}_{\mathrm{chp},j,t} + P^{\mathrm{g}}_{\mathrm{FN},j,t}, \forall j \in \Omega_{\mathrm{EH}}, \forall t. \tag{42}$$

3.3. Linearization of natural gas transmission model

Nonlinear constraints (25)–(27) can be transformed into a linear form by piecewise linearization, then the original planning model is reformulated into an MILP. Refer to [28] for the linearization procedure. Then constraints (17) and (25)–(30) can be replaced by (43)–(52).

$$GF_{p,t} = w_p(PI_{\mathrm{e},t} - PI_{\mathrm{s},t}), \forall p \in \Omega_{\mathrm{EP}}, \forall t, \tag{43}$$

$$GF_{p,t} - w_p(PI_{\mathrm{e},t} - PI_{\mathrm{s},t}) - M_{\mathrm{G}}(1 - z_p) \le 0, \forall p \in \Omega_{\mathrm{CP}}, \forall t, \tag{44}$$

$$-GF_{p,t} + w_p(PI_{\mathrm{e},t} - PI_{\mathrm{s},t}) - M_{\mathrm{G}}(1 - z_p) \le 0, \forall p \in \Omega_{\mathrm{CP}}, \forall t, \tag{45}$$

$$GF_{p,t} = GF_{p,t,1} + \sum_{k=1}^{seg} \delta_{p,t,k}(GF_{p,t,k+1} - GF_{p,t,k}), \forall p \in \Omega_{\mathrm{EP}} \cup \Omega_{\mathrm{CP}}, \forall t, \tag{46}$$

$$gf_{p,t} = gf_{p,t,1} + \sum_{k=1}^{seg} \delta_{p,t,k}(gf_{p,t,k+1} - gf_{p,t,k}), \forall p \in \Omega_{\mathrm{EP}} \cup \Omega_{\mathrm{CP}}, \forall t, \tag{47}$$

$$\delta_{p,t,k+1} \le \phi_{p,t,k}, k = 1, 2, \dots, seg, \forall p \in \Omega_{\mathrm{EP}} \cup \Omega_{\mathrm{CP}}, \forall t, \tag{48}$$

$$\phi_{p,t,k} \le \delta_{p,t,k}, k = 1, 2, \dots, seg + 1, \forall p \in \Omega_{\mathrm{EP}} \cup \Omega_{\mathrm{CP}}, \forall t, \tag{49}$$

$$0 \le \delta_{p,t,k} \le 1, k = 1, 2, \dots, seg + 1, \forall p \in \Omega_{\mathrm{EP}} \cup \Omega_{\mathrm{CP}}, \forall t, \tag{50}$$

$$\underline{PI}_m \le PI_{m,t} \le \overline{PI}_m, \forall m \in \Omega_{\mathrm{GN}}, \forall t, \tag{51}$$

$$\underline{PI}_{\mathrm{e},t} \le \varsigma_c^2 PI_{\mathrm{s},t}, \forall c \in \Omega_{\mathrm{COM}}, \forall t, \tag{52}$$

where subscript s represents the start node of corresponding existing and candidate pipelines or compressors, and subscript e represents end node. PI and GF are auxiliary variables to replace the nonlinear terms π^2 and $gf|gf|$. Auxiliary variables δ and ϕ (binary) bundle GF and gf together in piecewise linearization procedure.

3.4. Centralized planning model

Then the centralized planning model can be formulated as:

$$\begin{aligned} \min & \sum_{l\in\Omega_{\mathrm{CL}}} LC_l \cdot z_l + \sum_{p\in\Omega_{\mathrm{CP}}} PC_p \cdot z_p \\ & + \sum_{\forall t}[\sum_{i\in\Omega_{\mathrm{GEN}}} (GC_i \cdot P^{\mathrm{e}}_{i,t} + SC_i \cdot v_{i,t}) + \sum_{w\in\Omega_{\mathrm{GW}}} NC_w \cdot P^{\mathrm{g}}_{w,t}] \\ & + \sum_{j\in\Omega_{\mathrm{EH}}}[\sum_{n\in\Omega_{\mathrm{EN}}} s^{\mathrm{e}}_{n,j} \cdot ELC_n + \sum_{m\in\Omega_{\mathrm{GN}}} s^{\mathrm{g}}_{m,j} \cdot GLC_m] \end{aligned} \tag{53}$$

$s.t.$ (1)–(16), (18)–(24), (28)–(29), (31)–(52).

The objective (53) is to minimize the total investment and operation cost. The first two terms represent the investment cost of transmission lines and gas pipelines. The third term represents the operation cost, which consists of the generation and startup cost of units and production cost of gas sources. The last term represents the investment cost of EHs. The decision variables include: investment variables of transmission lines and gas pipelines, siting variables of EHs, commitment and production of generators, production of gas sources.

Constraints include the electric system constraints, natural gas system constraints and EH constraints. Electric system constraints consist of UC constraints (31)–(36), the nodal power balance (9), DC power flow and capacity constraints for existing and candidate transmission lines (10)–(14), and the phase angle constraint (15). Natural gas system constraints consist of natural gas source constraints (16), compressor constraints (18) and (52), gas storage constraints (19)–(23), the nodal gas load balance (24), capacity constraints for the existing and candidate gas pipelines(28) and (29), linearized Weymouth steady-state gas transmission constraints and capacity constraints for existing and candidate pipelines (43)–(50) and the nodal pressure constraint (51). EH constraints consist of energy conversion constraints of components (1)–(5), the multi-energy load balance on output port (6)–(8) and siting constraints for EHs (37)–(42).

4. Distributed IES planning

ADMM is adopted to relax the energy balance constraints at the nodes where EHs are connected to the electric system and gas system, and decompose the synergic planning into the electric network planning $\mathbf{SP}_{\mathrm{e}}$, the natural gas system planning $\mathbf{SP}_{\mathrm{g}}$ and n EHs siting $\mathbf{SP}_{\mathrm{eh},j}$, $j \in [1, n]$ to achieve an (n+2)-stakeholder distributed planning framework, in which each sub-problem is solved iteratively.

4.1. Coupling variables assignment of ADMM

The binary variables that represent the site of the EHs cannot be directly defined as coupling variables to update the Lagrangian multiplier by gradient ascent in ADMM framework due to its discreteness. In this paper, continuous variables of EHs $\mathbf{P}^{\mathrm{hfe}} \in \mathbb{R}^{n_{\mathrm{e}}\times n_{\mathrm{EH}}\times \mathrm{T}}$ and $\mathbf{P}^{\mathrm{hfg}} \in \mathbb{R}^{n_{\mathrm{g}}\times n_{\mathrm{EH}}\times \mathrm{T}}$, which represent the electricity and natural gas consumption of all EHs from each node of the electric and gas system, are assigned as coupling variables. The corresponding coupling variables in the electric and natural systems are $\mathbf{P}^{\mathrm{eth}} \in \mathbb{R}^{n_{\mathrm{e}}\times n_{\mathrm{EH}}\times \mathrm{T}}$ and $\mathbf{P}^{\mathrm{gth}} \in \mathbb{R}^{n_{\mathrm{e}}\times n_{\mathrm{EH}}\times \mathrm{T}}$, which represent the electricity and gas that the corresponding systems provide for EHs in each node.

The information exchange in the ADMM framework can be looked upon as being processed by the coordinators between the electric system and EHs (CoEH), as well as between the gas system and EHs (CoGH), who update the values of coupling variables and Lagrangian multipliers of each stakeholder. As such, consensus variables $\mathbf{Pn}^{\mathrm{e}} \in \mathbb{R}^{n_{\mathrm{e}}\times n_{\mathrm{EH}}\times \mathrm{T}}$ and $\mathbf{Pn}^{\mathrm{g}} \in \mathbb{R}^{n_{\mathrm{e}}\times n_{\mathrm{EH}}\times \mathrm{T}}$ need to be introduced to represent the synergy between the EHs and the electric system, and between the EHs and the natural gas system, respectively, which represent the coupling variables after the coordination in CoEH and CoGH:

$$\mathbf{P}^{\mathrm{eth}} - \mathbf{Pn}^{\mathrm{e}} = 0, \mathbf{P}^{\mathrm{hfe}} - \mathbf{Pn}^{\mathrm{e}} = 0, \tag{54}$$

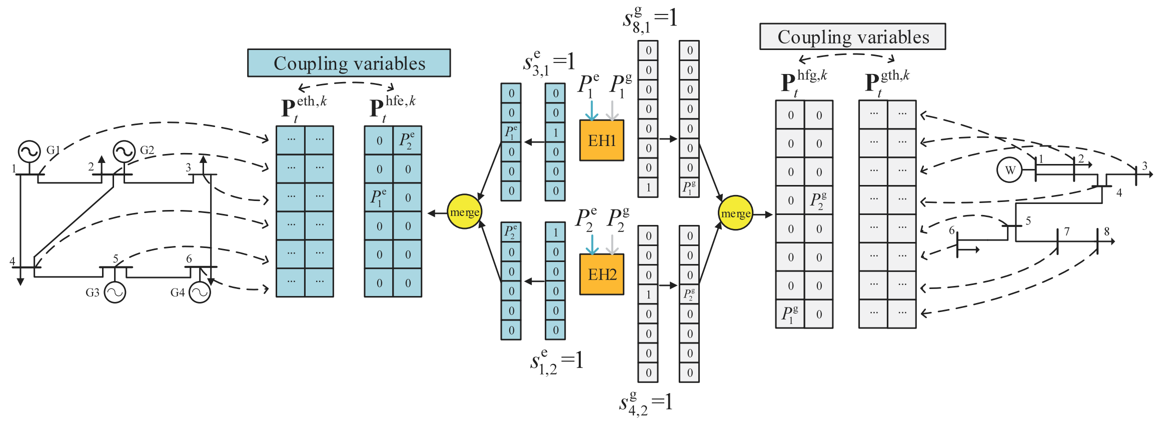

Fig. 3. The coupling variables of the distributed IES network planning model in hour t.

$$\mathbf{P}^{\mathrm{gth}} - \mathbf{Pn}^{\mathrm{g}} = 0, \mathbf{P}^{\mathrm{hfg}} - \mathbf{Pn}^{\mathrm{g}} = 0, \tag{55}$$

$\mathbf{P}^{\mathrm{eth}}$ and $\mathbf{P}^{\mathrm{hfe}}$, $\mathbf{P}^{\mathrm{eth}}$ and $\mathbf{P}^{\mathrm{hfg}}$ are bundled by $\mathbf{Pn}^{\mathrm{e}}$ and $\mathbf{Pn}^{\mathrm{g}}$ in (54) and (55), which guarantee the energy balance of nodes that EHs are connected to.

The distributed decision making is graphed in Fig. 3, which shows the coupling variable matrices. Each entry in the coupling variable matrices represents the energy flow between the different systems with its column index j representing the jth EH and row index n representing the nth node in the electric or gas system. Each column of the coupling variable matrices $\mathbf{P}_t^{\mathrm{hfe}}$ and $\mathbf{P}_t^{\mathrm{hfg}}$ then has only one non-zero entry indicating that each EH can only be connected to only one single node in the electric and gas system at most as constrained by (37) and (40). The sum of each row represents the amount of electricity or natural gas that the systems provide for the EHs through the corresponding nodes. For example, in Fig. 3 EH1 is determined to connect to node 3 of the electric system and node 8 of the natural gas system since $s_{3,1}^{\mathrm{e}} = 1$ and $s_{8,1}^{\mathrm{g}} = 1$, respectively, and EH1 intends to obtain P_1^{e} from node 3 of the electric system, and P_1^{g} from node 8 of the gas system in hour t.

Each stakeholder maximizes its own benefits independently in distributed optimization, which might lead to the inability to reach an agreement on the value of coupling variables, and it is mathematically denoted as violating (54)–(55). Therefore, each stakeholder needs to adjust its decision according to the coupling variables given by others. This negotiation process is imitated by the iteration of ADMM, and the negotiation target is the convergence condition of ADMM. Then the sub-problems are formulated as follow.

(1) Electricity network planning problem $\mathbf{SP}_{\mathrm{e}}$: The objective of the electricity network planning sub-problem can be formulated by adding the Lagrange relaxation term and regularization term to the electric investment and operation cost in (53):

$$\begin{aligned}\min & \sum_{\forall t}\sum_{i\in\Omega_{\mathrm{GEN}}} GC_i \cdot P_{i,t}^{\mathrm{e}} + \sum_{\forall t}\sum_{i\in\Omega_{\mathrm{GEN}}} SC_i \cdot v_{i,t} + \sum_{l\in\Omega_{\mathrm{CL}}} LC_l \cdot z_l \\ & + \sum_{\forall t}\sum_{j\in\Omega_{\mathrm{EH}}}\sum_{n\in\Omega_{\mathrm{EN}}} \lambda_{n,j,t}^{\mathrm{e},k}\left(P_{n,j,t}^{\mathrm{eth},k+1} - Pn_{n,j,t}^{\mathrm{e},k}\right) \\ & + \frac{\rho_{\mathrm{e}}}{2}\sum_{\forall t}\sum_{j\in\Omega_{\mathrm{EH}}}\sum_{n\in\Omega_{\mathrm{EN}}}\left(P_{n,j,t}^{\mathrm{eth},k+1} - Pn_{n,j,t}^{\mathrm{e},k}\right)^2\end{aligned} \tag{56}$$

s.t. (10)–(15), (31)–(36), (57).

$$\sum_{i\in\Omega_{\mathrm{GEN}}} A_{n,i}P_{i,t}^{\mathrm{e}} - \sum_{j\in\Omega_{\mathrm{EH}}} P_{n,j,t}^{\mathrm{eth}} - L_{n,t}^{\mathrm{e}} + \sum_{l\in\Omega_{\mathrm{EL}}} B_{n,l}pf_{l,t} + \sum_{l\in\Omega_{\mathrm{CL}}} B_{n,l}pf_{l,t} = 0, \forall n \in \Omega_{\mathrm{EN}}, \forall t, \tag{57}$$

where (57) is the reformulated nodal power balance constraint in the electricity network planning sub-problem, and (56) is the objective that ensures the electric system make the most economic investment and operation decisions, given the electricity consumption of EHs after the kth iteration. Then the coupling variable $\mathbf{P}^{\mathrm{eth},k+1}$ will be passed to CoEH for the (k+1) th iteration.

(2) Natural gas system planning problem $\mathbf{SP}_{\mathrm{g}}$:

$$\begin{aligned}\min & \sum_{\forall t}\sum_{w\in\Omega_{\mathrm{GW}}} NC_w \cdot P_{w,t}^{\mathrm{g}} + \sum_{p\in\Omega_{\mathrm{CP}}} PC_p \cdot z_p \\ & + \sum_{\forall t}\sum_{j\in\Omega_{\mathrm{EH}}}\sum_{m\in\Omega_{\mathrm{GN}}} \lambda_{m,j,t}^{\mathrm{g},k}\left(P_{m,j,t}^{\mathrm{gth},k+1} - Pn_{m,j,t}^{\mathrm{g},k}\right) \\ & + \frac{\rho_{\mathrm{g}}}{2}\sum_{\forall t}\sum_{j\in\Omega_{\mathrm{EH}}}\sum_{m\in\Omega_{\mathrm{GN}}}\left(P_{m,j,t}^{\mathrm{gth},k+1} - Pn_{m,j,t}^{\mathrm{g},k}\right)^2\end{aligned} \tag{58}$$

s.t. (16), (18)–(23), (28)–(29), (43)–(52), (59).

Similar to the electric system planning, (59) is the reformulated nodal gas load balance constraint from (24):

$$\begin{aligned}& \sum_{w\in\Omega_{\mathrm{GAS}}} C_{m,w}P_{w,t}^{\mathrm{g}} - \sum_{j\in\Omega_{\mathrm{EH}}} P_{m,j,t}^{\mathrm{gth}} - L_{m,t}^{\mathrm{g}} + \sum_{p\in\Omega_{\mathrm{EP}}} D_{m,p}gf_{p,t} + \sum_{p\in\Omega_{\mathrm{CP}}} D_{m,p}gf_{p,t} + \\ & \sum_{c\in\Omega_{\mathrm{COM}}} H_{m,c}cf_{c,t} + \sum_{s\in\Omega_{\mathrm{GS}}} J_{m,s}\left(P_{s,t}^{\mathrm{dc}} - P_{s,t}^{\mathrm{ch}}\right) = 0, \forall m \in \Omega_{\mathrm{GN}}, \forall t.\end{aligned} \tag{59}$$

(3) EH planning problem $\mathbf{SP}_{\mathrm{eh},j}$ ($j \in \Omega_{\mathrm{EH}}$): EH is modeled as a single stakeholder. For EH j, the objective function is:

$$\begin{aligned}\min & \sum_{n\in\Omega_{\mathrm{EN}}} s_{n,j}^{\mathrm{e}} \cdot ELC_n + \sum_{m\in\Omega_{\mathrm{GN}}} s_{m,j}^{\mathrm{g}} \cdot GLC_m \\ & + \sum_{\forall t}\sum_{n\in\Omega_{\mathrm{EN}}} \lambda_{n,j,t}^{\mathrm{he},k}\left(P_{n,j,t}^{\mathrm{hfe},k+1} - Pn_{n,j,t}^{\mathrm{e},k}\right) + \frac{\rho_{\mathrm{he}}}{2}\sum_{\forall t}\sum_{n\in\Omega_{\mathrm{EN}}}\left(P_{n,j,t}^{\mathrm{hfe},k+1} - Pn_{n,j,t}^{\mathrm{e},k}\right)^2 \\ & + \sum_{\forall t}\sum_{m\in\Omega_{\mathrm{GN}}} \lambda_{m,j,t}^{\mathrm{hg},k}\left(P_{m,j,t}^{\mathrm{hfg},k+1} - Pn_{m,j,t}^{\mathrm{g},k}\right) + \frac{\rho_{\mathrm{hg}}}{2}\sum_{\forall t}\sum_{m\in\Omega_{\mathrm{GN}}}\left(P_{m,j,t}^{\mathrm{hfg},k+1} - Pn_{m,j,t}^{\mathrm{g},k}\right)^2\end{aligned}$$

s.t. (1)–(8), (37)–(42).

$$\tag{60}$$

There are n separate entities for n EHs. Therefore, the IES incorporating district EHs planning model has (n+2) entities.

4.2. Solution procedure

The (n+2) sub-problems are solved in parallel by ADMM. The solution procedure is put in detail below, which aligns all variables with the same period, and has hence leaves out the subscript t for simplicity, e.g., λ^{e} for $\lambda_{\mathbf{t}}^{\mathbf{e}}$.

Step 1. The CoEH and CoGH initialize $\lambda^{\mathbf{he}}$, $\lambda^{\mathbf{hg}}$, λ^{e}, λ^{g}, $\mathbf{Pn}^{\mathbf{e}}$, $\mathbf{Pn}^{\mathbf{g}}$ and send them to the electric system, gas system and EHs.

Step 2. Each stakeholder solves their sub-problem and returns the coupling variables to CoEH and CoGH in parallel:

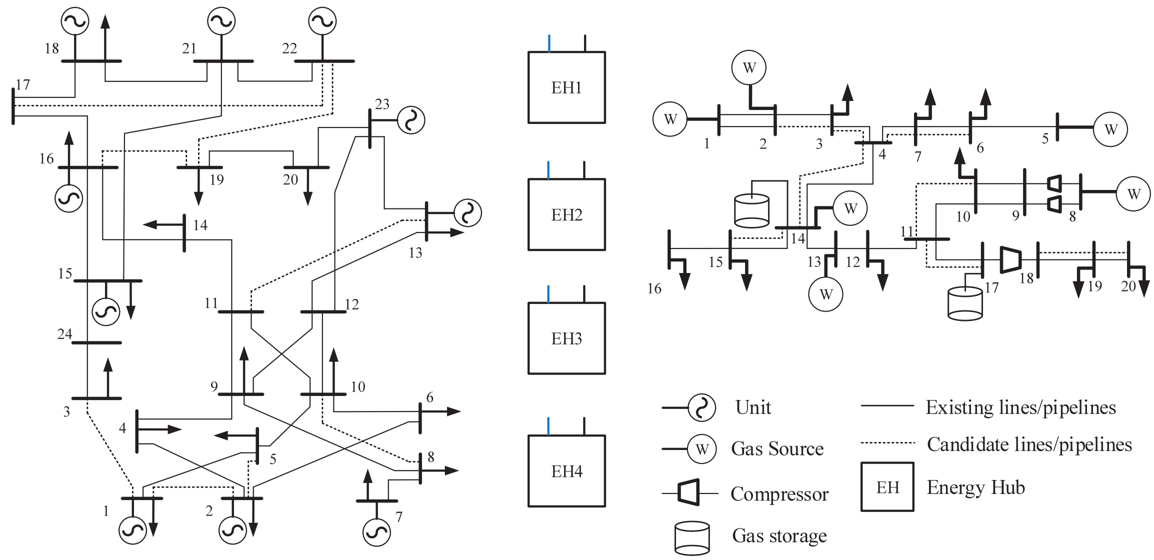

Fig. 4. An IES composed of modified IEEE RTS 24-bus system, Belgian 20-node natural gas system and four district EHs.

- electric system solves $\mathbf{SP}_{\mathrm{e}}$ to obtain the power that can be supplied to each node in every hour by power system $\mathbf{P}^{\mathrm{eth},k+1}$ after receiving the coupling variable $\mathbf{Pn}^{\mathrm{e},k}$ and sends it back to CoEH;
- gas system solves $\mathbf{SP}_{\mathrm{g}}$ to obtain the natural gas that can be supplied to each node in every hour by gas system $\mathbf{P}^{\mathrm{gth},k+1}$ after receiving the coupling variable $\mathbf{Pn}^{\mathrm{g},k}$ and sends it back to CoGH;
- EH j ($j \in \Omega_{\mathrm{EH}}$) solves $\mathbf{SP}_{\mathrm{eh},j}$ to obtain $\mathbf{P}_j^{\mathrm{hfe},k+1}$ and $\mathbf{P}_j^{\mathrm{hfg},k+1}$ (The jth column of $\mathbf{P}^{\mathrm{hfe}}$ and $\mathbf{P}^{\mathrm{hfg}}$) and sends them back to CoEH and CoGH.

Step 3. CoEH and CoGH update the consensus variables by taking the average value of the coupling variables of different stakeholders via (61)–(62) and check if the stopping criteria (63)–(66) is satisfied. If yes, the iteration converges. Otherwise, update the Lagrangian multipliers by (67)–(70) and go back to step2 until it converges.

$$\mathbf{Pn}^{\mathrm{e},k+1} = 0.5 \times (\mathbf{P}^{\mathrm{hfe},k+1} + \mathbf{P}^{\mathrm{eth},k+1}), \tag{61}$$

$$\mathbf{Pn}^{\mathrm{g},k+1} = 0.5 \times (\mathbf{P}^{\mathrm{hfg},k+1} + \mathbf{P}^{\mathrm{gth},k+1}), \tag{62}$$

$$\max_{\forall j\in\Omega_{\mathrm{EH}},\forall n\in\Omega_{\mathrm{EN}},\forall t} (|P_{n,j,t}^{\mathrm{eth},k+1} - Pn_{n,j,t}^{\mathrm{e},k+1}|, |P_{n,j,t}^{\mathrm{hfe},k+1} - Pn_{n,j,t}^{\mathrm{e},k+1}|) \le \varepsilon_{\mathrm{e}}, \tag{63}$$

$$\max_{\forall j\in\Omega_{\mathrm{EH}},\forall n\in\Omega_{\mathrm{EN}},\forall t} (\rho_{\mathrm{e}}|P_{n,j,t}^{\mathrm{eth},k+1} - P_{n,j,t}^{\mathrm{eth},k}|, \rho_{\mathrm{he}}|P_{n,j,t}^{\mathrm{hfe},k+1} - P_{n,j,t}^{\mathrm{hfe},k}|) \le \varepsilon_{\mathrm{e}}, \tag{64}$$

$$\max_{\forall j\in\Omega_{\mathrm{EH}},\forall m\in\Omega_{\mathrm{GN}},\forall t} (|P_{m,j,t}^{\mathrm{gth},k+1} - Pn_{m,j,t}^{\mathrm{g},k+1}|, |P_{m,j,t}^{\mathrm{hfg},k+1} - Pn_{m,j,t}^{\mathrm{g},k+1}|) \le \varepsilon_{\mathrm{g}}, \tag{65}$$

$$\max_{\forall j\in\Omega_{\mathrm{EH}},\forall m\in\Omega_{\mathrm{GN}},\forall t} (\rho_{\mathrm{g}}|P_{m,j,t}^{\mathrm{gth},k+1} - P_{m,j,t}^{\mathrm{gth},k}|, \rho_{\mathrm{hg}}|P_{m,j,t}^{\mathrm{hfg},k+1} - P_{m,j,t}^{\mathrm{hfg},k}|) \le \varepsilon_{\mathrm{g}}, \tag{66}$$

$$\lambda^{\mathrm{he},k+1} = \lambda^{\mathrm{he},k} + \rho_{\mathrm{he}} \times (\mathbf{P}^{\mathrm{hfe},k+1} - \mathbf{Pn}^{\mathrm{e},k+1}), \tag{67}$$

$$\lambda^{\mathrm{e},k+1} = \lambda^{\mathrm{e},k} + \rho_{\mathrm{e}} \times (\mathbf{P}^{\mathrm{eth},k+1} - \mathbf{Pn}^{\mathrm{e},k+1}), \tag{68}$$

$$\lambda^{\mathrm{hg},k+1} = \lambda^{\mathrm{hg},k} + \rho_{\mathrm{hg}} \times (\mathbf{P}^{\mathrm{hfg},k+1} - \mathbf{Pn}^{\mathrm{g},k+1}), \tag{69}$$

$$\lambda^{\mathrm{g},k+1} = \lambda^{\mathrm{g},k} + \rho_{\mathrm{g}} \times (\mathbf{P}^{\mathrm{gth},k+1} - \mathbf{Pn}^{\mathrm{g},k+1}). \tag{70}$$

The (n+2) sub-problems each composed of variables defined on all time periods are solved in each iteration of ADMM, hence return results of all periods simultaneously when it converges. Though the rigorous convergence and its proof are beyond the scope of this paper, common convergence to a feasible and suboptimal solution in the ADMM application is observed in the problem herein.

Table 1
Parameters of EH components.

EH components	η	Capacity/MW
CHP	$\eta_{\mathrm{chp}}^{\mathrm{ge}} = 0.6$, $\eta_{\mathrm{chp}}^{\mathrm{gh}} = 0.45$,	300
EB	$\eta_{\mathrm{boi}}^{\mathrm{eh}} = 0.75$	200
P2G	$\eta_{\mathrm{p2g}}^{\mathrm{eg}} = 0.8$	200

Table 2
Parameters of candidate transmission lines.

Start node	End node	b_l/s	$\overline{pf}_l$/MW	Cost/10^4\$
1	2	0.000139	175	7.35
1	3	0.001651	175	4.25
2	5	0.001267	175	3.50
11	13	0.000476	500	5.31
16	19	0.001053	500	5.11
19	22	0.000396	500	5.70

Table 3
Parameters of candidate pipelines.

Start node	End node	w_p	$\underline{gf}_p$/MSCM·h^{-1}	$\overline{gf}_p$/MSCM·h^{-1}	Cost/10^4\$
2	3	1.395	0	10	4.20
6	7	0.148	−6	0	5.10
4	14	0.659	0	10	6.00
10	11	0.226	0	5	4.50
14	15	3.628	0	25	7.50
11	17	0.051	0	5	3.50
18	19	0.002	0	5	3.50
19	20	0.028	0	4	4.00

5. Case study

The IES shown in Fig. 4 integrating the modified IEEE RTS 24-bus electric system [29], Belgian 20-node natural gas system [30] and four EHs is used to verify the effectiveness of the proposed distributed planning model, with data available in [29] and [30]. The parameters of EHs' components, candidate transmission lines and gas pipelines and investment cost of EHs in each node are given in Tables 1–4, while the configuration of the EHs is given in Fig. 1. The mixed integer linear programs of both the centralized synergistic planning and the ADMM-based distributed planning are solved by CPLEX 12.8.0. Parameters ε_{e} and ε_{g} are both set to 0.001, ρ_{e} is set to 100, ρ_{he} is set to 20, ρ_{g} is set to 800, ρ_{hg} is set to 400, and the number of segments of the linearization of natural gas transmission function is set to 3.

Table 4
Investment cost of EHs in electric nodes and gas nodes.

EN	Cost/10^4\$	EN	Cost/10^4\$	EN	Cost/10^4\$	GN	Cost/10^4\$	GN	Cost/10^4\$	GN	Cost/10^4\$
3	7.75	4	10.70	2	12.00	17	6.50	3	9.20	4	13.10
10	8.13	22	11.00	8	12.25	11	6.90	1	9.75	18	13.35
11	8.34	21	11.30	18	12.31	5	7.20	6	10.80	7	14.40
6	8.85	14	11.50	23	12.38	2	7.50	20	11.00	8	15.00
20	8.91	7	11.80	15	12.40	10	7.75	16	11.35		
24	8.97	13	11.65	12	12.50	12	7.90	9	11.50		
17	9.10	16	11.85	9	12.80	13	8.25	14	12.00		
1	10.00	5	11.92	19	13.00	15	8.75	19	13.00		

Table 5
Planning scheme of the two planning approaches.

	Centralized planning	ADMM-based planning
Electric system	lines: 16–19, 11–13	lines: 1–3, 16–19, 11–13
Natural gas system	pipelines: 2–3, 4–14, 10–11, 18–19	pipelines: 2–3, 4–14, 10–11, 18–19
EH1	SE: 10, SG: 11	SE: 10, SG: 5
EH2	SE: 20, SG: 2	SE: 3, SG: 2
EH3	SE: 7, SG: 5	SE: 24, SG: 11
EH4	SE: 22, SG: 11	SE: 22, SG: 11

Table 6
Cost of the two planning approaches.

	Centralized planning/10^4\$	ADMM-based planning/10^4\$
O_c of the electric system	32.44	31.40
I_c of the electric system	10.42	14.67
O_c of the natural gas system	22.56	23.81
I_c of the natural gas system	18.20	18.20
I_c of EH1	15.03	15.33
I_c of EH2	16.41	15.25
I_c of EH3	19.00	15.87
I_c of EH4	17.90	17.90
Total cost	151.96	152.43(+0.31%)

5.1. Effectiveness of distributed planning model

The proposed ADMM-based distributed planning model is compared with the centralized synergic model. The detailed planning scheme obtained by the two approaches are shown in Table 5 (SE represents the site in the electric system, and SG represents the site in the gas system), while their investment and operation costs are shown in Table 6, in which O_c and I_c represent the operation cost and investment cost, respectively.

Decisions reached by the two approaches are similar. Obviously, the investment decision of the natural gas system in the two planning approaches are the same with each other, and the nodes selected by EHs in the gas system are the same as well. The only difference occurs at the nodes selected by EHs in the electric system, and the investment of a single transmission line. EH2 is sited to node 3 of the electric system by the distributed model, which urges the electric system to build line 1–3 to transmit electricity from node 1 to node 3 to satisfy the electricity consumption of EH2.

The investment and operation cost of the two planning approaches are close as shown in Table 6. It is assumed that there is a single stakeholder in the centralized planning model who possesses all the information of the whole IES to make investment and operation decisions and is then able to directly solve for the global optimal solution. In contrast, the proposed distributed planning model classifies the electric system, gas system and EHs as separate stakeholders, and obtains a total cost 0.31% larger than the global optimal solution. This is because each stakeholder in the distributed planning model adjusts its investment and operation strategy according to the value of coupling variables passed by other stakeholders. And the difference of the value of coupling variables diminishes in the iteration of ADMM algorithm until it converges. That is, each stakeholder achieves a consensus in the negotiation and this approach guarantees feasibility.

In summary, the proposed ADMM-based distributed planning model not only ensures the decision independence of the electric system, the gas system and EHs, but also achieves benefits for the multiple stakeholders simultaneously by obtaining an investment and operation strategy close to the global optimal solution. As such, the proposed distributed planning model has its effectiveness verified.

Table 7
Units status of the two cases.

UC-embedded	unit1	∘	∘	∘	∘	∘	∘	•	•	•	•	•	•	•	•	•	•	•	•	•	•	•	•	∘	∘
	unit6	∘	∘	∘	∘	∘	∘	∘	∘	∘	∘	∘	∘	∘	∘	∘	∘	∘	∘	∘	∘	∘	∘	∘	∘
	unit7	∘	∘	∘	∘	∘	∘	∘	∘	∘	•	•	•	•	•	•	•	•	•	•	•	•	∘	∘	∘
Non-UC	unit1	∘	∘	∘	∘	∘	∘	•	•	•	•	•	•	•	•	•	•	•	•	∘	∘	•	•	∘	∘
	unit6	∘	∘	∘	∘	∘	∘	∘	∘	∘	∘	•	∘	∘	∘	∘	∘	∘	∘	•	•	∘	∘	∘	∘
	unit7	∘	∘	∘	∘	∘	∘	∘	∘	•	•	•	•	•	∘	∘	∘	∘	•	•	•	•	∘	∘	∘

5.2. The impact of UC

A distributed IES planning model embedded with the single period optimal power flow is performed as a baseline to highlight the advantage of the UC-embedded planning model in better accounting for the operation status of units.

The resulting units' status are given in Table 7, in which • represents that units are online and ∘ means that units are offline. Clearly, in the non-UC case, unit 6 is online for only an hour in hour 11, unit 1 is only offline for consecutive two hours in hour 19 and 20, which violates the minimum up and downtime constraints. In addition, redundant units would be kept online in the scheduling or multiple period optimal power flow embedded traditional planning model, which leads to less economical operation schemes than the UC-embedded planning. In summary, the proposed UC-embedded planning can more accurately model the system operation in the planning to attain higher economic efficiency.

Table 8
The different siting strategies and total production of all units caused by different multipliers for the gas price.

Multipliers		0.1	0.5	1	2	5
EH1	SE	–	17	10	13	13
	SG	9	5	5	17	17
EH2	SE	3	3	3	22	22
	SG	9	9	2	5	–
EH3	SE	6	6	24	24	24
	SG	11	11	11	11	11
EH4	SE	10	10	22	13	18
	SG	5	9	11	17	17
Total production of all units/$\times 10^4$MW		4.517	4.753	5.627	6.795	6.909

Table 9
The different number of iteration resulting from different multipliers for the penalty factors.

Multipliers	The number of iterations
0.5	225
1	143
2	101
3	130
5	Not converge

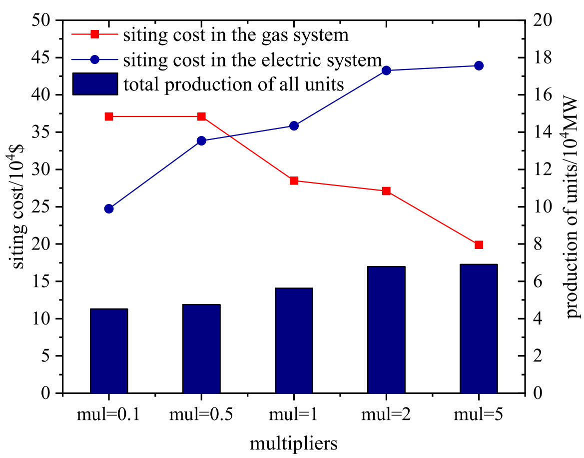

Fig. 5. The different siting costs and total production of all units caused by different multipliers for the gas price..

5.3. *The impact of natural gas price*

Gas price is altered to show the impact of boundary conditions on the planning strategy, and the different siting decisions and total production of all units resulting from the gas price with different multipliers are shown in Table 8 and Fig. 5. The total production of all units grows as the natural gas price increases. When the gas price is 5 times of that in the basic model, EH2 is then determined not to connect to gas system indicating that it is cheaper to supply its heat load by the electric boiler rather than CHP. And its obvious in Fig. 5 that the EHs tend to connect to the nodes that have lower siting cost in the gas system as the gas price increases because of less natural gas consumption. Similarly, for a low gas price (one tenth of basic model), EH1 is determined not to connect to electric system indicating that it is cheaper to supply the heat and electric load by CHP rather than electric system and electric boiler, and the EHs tend to connect to the nodes that have lower siting cost in the electric system as the gas price decreases resulting from less electricity consumption.

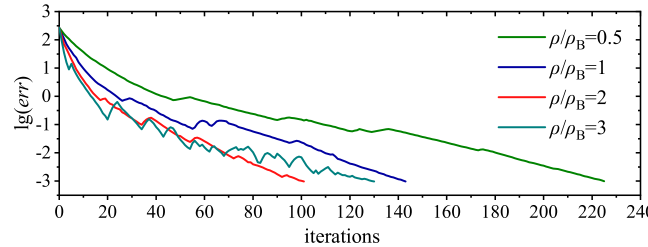

Fig. 6. Evolution of primal residual errors resulting from different multipliers for penalty factors.

5.4. *The impact of penalty parameters*

The different number of iterations and the evolution of primal residual errors (*err* in Fig. 6) resulting from different multipliers for the penalty parameters ρ (ρ_e, ρ_{he}, ρ_g and ρ_{hg}) are shown in Table 9 and Fig. 6. The minimum number of iterations is 101 when the penalty parameters are 2 times of that from the basic setting. The number of iterations increases as the value of penalty parameters decreases because of the smaller iteration step in the multipliers update. However, oscillations will be introduced in the multipliers update when the step size gets too large, so the number of iterations increases when the value of penalty parameters are larger than 2 times of that from the basic setting, and ADMM cannot converge when they are 5 times of that from the basic setting.

6. Conlusion

To achieve independent decision-making of the electric system, the natural gas system and district EHs in the synergic planning of them, this paper proposes an ADMM-based distributed multi-energy network planning and EHs siting model with the object of minimizing the investment and operation cost, in which the three systems are assigned as separate stakeholders. To smooth the update of the Lagrangian multipliers of ADMM, a novel modeling is proposed to relax the continuous electricity and gas balance constraints at each EH-node interface instead of binary EH siting constraints. To more accurately represent the system operation in the planning framework and improve the operational flexibility, UC is embedded in the proposed distributed planning framework. Case studies performed on an IES composed of a modified IEEE RTS 24-bus electric system, the Belgian 20-node natural gas system and four district EHs show that: (1) the planning results obtained by the distributed planning are close to the global optimum obtained by the centralized planning, which verifies the efficiency of the proposed (n+2)-agent distributed planning framework; and (2) compared with the single/multi-period optimal power flow, UC models the system operation more accurately in the planning stage, which helps improve the economy of the plan.

CRediT authorship contribution statement

Hangbo Yang: Software, Data curation, Investigation, Writing - original draft. **Pengcheng You:** Methodology, Writing - review & editing. **Ce Shang:** Conceptualization, Methodology, Supervision, Resources, Writing - review & editing.

Declaration of competing interest

The authors declare that they have no known competing financial interests or personal relationships that could have appeared to influence the work reported in this paper.

Acknowledgments

The authors would like to thank the National Natural Science Foundation of China for Grant 51807115, the Shanghai Sailing Program by the Science and Technology Commission of Shanghai Municipality under Grant 18YF1411400, and the Young Elite Scientists Sponsorship Program by the Chinese Society of Electrical Engineers under Grant CSEE-YESS-2018016.

References

[1] Farrokhifar M, Nie Y, Pozo D. Energy systems planning: A survey on models for integrated power and natural gas networks coordination. Appl Energy 2020;262:114567. http://dx.doi.org/10.1016/j.apenergy.2020.114567.

[2] Wang Y, Wang Y, Huang Y, Yang J, Ma Y, et al. Operation optimization of regional integrated energy system based on the modeling of electricity-thermal-natural gas network. Appl Energy 2019;251:113410. http://dx.doi.org/10.1016/j.apenergy.2019.113410.

[3] Wang C, Lv C, Li P, Song G, Li S, et al. Modeling and optimal operation of community integrated energy systems: A case study from China. Appl Energy 2018;230:1242–54. http://dx.doi.org/10.1016/j.apenergy.2018.09.042.

[4] Zhang X, Shahidehpour M, Alabdulwahab A, Abusorrah A. Optimal expansion planning of energy hub with multiple energy infrastructures. IEEE Trans Smart Grid 2015;6(5):2302–11. http://dx.doi.org/10.1109/TSG.2015.2390640.

[5] Huang W, Zhang N, Dong R, Liu Y, Kang C. Coordinated planning of multiple energy networks and energy hubs (in Chinese with an extended summary in English). Proc CSEE 2018;38(18):5425–37. http://www.pcsee.org/CN/abstract/abstract30789.shtml.

[6] Cheng Y, Zhang N, Kirschen DS, Huang W, Kang C. Planning multiple energy systems for low-carbon districts with high penetration of renewable energy: An empirical study in China. Appl Energy 2020;261:114390. http://dx.doi.org/10.1016/j.apenergy.2019.114390.

[7] Unsihuay-Vila C, Marangon-Lima JW, de Souza ACZ, Perez-Arriaga IJ, Balestrassi PP. A model to long-term, multiarea, multistage, and integrated expansion planning of electricity and natural gas systems. IEEE Trans Power Syst 2010;25(2):1154–68. http://dx.doi.org/10.1109/TPWRS.2009.2036797.

[8] Zeng Q, Zhang B, Fang J, Chen Z. A bi-level programming for multistage co-expansion planning of the integrated gas and electricity system. Appl Energy 2017;200:192–203. http://dx.doi.org/10.1016/j.apenergy.2017.05.022.

[9] Zhao B, Conejo AJ, Sioshansi R. Coordinated expansion planning of natural gas and electric power systems. IEEE Trans Power Syst 2018;33(3):3064–75. http://dx.doi.org/10.1109/TPWRS.2017.2759198.

[10] Ding T, Hu Y, Bie Z. Multi-stage stochastic programming with nonanticipativity constraints for expansion of combined power and natural gas systems. IEEE Trans Power Syst 2018;33(1):317–28. http://dx.doi.org/10.1109/TPWRS.2017.2701881.

[11] Liang J, Tang W. Stochastic multistage co-planning of integrated energy systems considering power-to-gas and the cap-and-trade market. Int J Electr Power Energy Syst 2020;119:105817. http://dx.doi.org/10.1016/j.ijepes.2020.105817.

[12] Zhou H, Zheng JH, Li Z, Wu QH, Zhou XX. Multi-stage contingency-constrained co-planning for electricity-gas systems interconnected with gas-fired units and power-to-gas plants using iterative benders decomposition. Energy 2019;180:689–701. http://dx.doi.org/10.1016/j.energy.2019.05.119.

[13] He C, Wu L, Liu T, Bie Z. Robust co-optimization planning of interdependent electricity and natural gas systems with a joint N-1 and probabilistic reliability criterion. IEEE Trans Power Syst 2018;33(2):2140–54. http://dx.doi.org/10.1109/TPWRS.2017.2727859.

[14] Shao C, Shahidehpour M, Wang X, Wang X, Wang B. Integrated planning of electricity and natural gas transportation systems for enhancing the power grid resilience. IEEE Trans Power Syst 2017;32(6):4418–29. http://dx.doi.org/10.1109/TPWRS.2017.2672728.

[15] Yan M, He Y, Shahidehpour M, Ai X, Li Z, Wen J. Coordinated regional-district operation of integrated energy systems for resilience enhancement in natural disasters. IEEE Trans Smart Grid 2019;10(5):4881–92. http://dx.doi.org/10.1109/TSG.2018.2870358.

[16] Wu C, Gu W, Xu Y, Jiang P, Lu S, Zhao B. Bi-level optimization model for integrated energy system considering the thermal comfort of heat customers. Appl Energy 2018;232:607–16. http://dx.doi.org/10.1016/j.apenergy.2018.09.212.

[17] Correa-Posada CM, Sánchez-Martın P. Security-constrained optimal power and natural-gas flow. IEEE Trans Power Syst 2014;29(4):1780–7. http://dx.doi.org/10.1109/TPWRS.2014.2299714.

[18] Wang X, Bie Z. Distributed co-planning of electricity and natural gas systems based on alternating direction method of multipliers (in Chinese). Autom Electr Power Syst 2018;42(22):107–17. http://dx.doi.org/10.7500/AEPS20180129011.

[19] Wen Y, Qu X, Li W, Liu X, Ye X. Synergistic operation of electricity and natural gas networks via ADMM. IEEE Trans Smart Grid 2018;9(5):4555–65. http://dx.doi.org/10.1109/TSG.2017.2663380.

[20] He C, Wu L, Liu T, Shahidehpour M. Robust co-optimization scheduling of electricity and natural gas systems via ADMM. IEEE Trans Sustain Energy 2017;8(2):658–70. http://dx.doi.org/10.1109/TSTE.2016.2615104.

[21] Wen Y, Qu X, Xiao Y, Yuan P. Distributed coordinated optimal dispatch of multi-regional electricity-gas integrated energy systems with energy hubs (in Chinese). Autom Electr Power Syst 2019;43(09):22–30. http://dx.doi.org/10.7500/AEPS20181007006.

[22] Cheng Y, Zhang N, Lu Z, Kang C. Planning multiple energy systems toward low-carbon society: A decentralized approach. IEEE Trans Smart Grid 2019;10(5):4859–69. http://dx.doi.org/10.1109/TSG.2018.2870323.

[23] Pan G, Gu W, Zhou S, Wu Z, Qiu H, Lu Y. Synchronously decentralized adaptive robust planning method for multi-stakeholder integrated energy systems. IEEE Trans Sustain Energy 2019;1. http://dx.doi.org/10.1109/TSTE.2019.2917921.

[24] Stephen B, Neal P, Eric C, Borja P, Jonathan E. Distributed optimization and statistical learning via the alternating direction method of multipliers. Foundations and Trends® in Machine Learning 2011;3(1):1–122. http://dx.doi.org/10.1561/2200000016.

[25] Koltsaklis NE, Georgiadis MC. A multi-period, multi-regional generation expansion planning model incorporating unit commitment constraints. Appl Energy 2015;158:310–31. http://dx.doi.org/10.1016/j.apenergy.2015.08.054.

[26] Hua B, Baldick R, Wang J. Representing operational flexibility in generation expansion planning through convex relaxation of unit commitment. IEEE Trans Power Syst 2018;33(2):2272–81. http://dx.doi.org/10.1109/TPWRS.2017.2735026.

[27] Morales-Espana G, Latorre JM, Ramos A. Tight and compact MILP formulation for the thermal unit commitment problem. IEEE Trans Power Syst 2013;28(4):4897–908. http://dx.doi.org/10.1109/TPWRS.2013.2251373.

[28] Markowitz H, Manne A. On the solution of discrete programming problems. Econometrica 1957;25. http://dx.doi.org/10.2307/1907744.

[29] Grigg C, Wong P, Albrecht P, Allan R, Bhavaraju M, et al. The IEEE reliability test system-1996. IEEE Trans Power Syst 1999;14(3):1010–20. http://dx.doi.org/10.1109/59.780914.

[30] De Wolf D, Smeers Y. The gas transmission problem solved by an extension of the simplex algorithm. Manage Sci 2000;46(11):1454–65. http://dx.doi.org/10.1287/mnsc.46.11.1454.12087.